

IR + VUV double resonance spectroscopy and extended density functional theory studies of ketone solvation by alcohol: 2-butanone-(methanol)_n, n = 1–4 clusters

Joong-Won Shin, and Elliot R. Bernstein

Citation: *The Journal of Chemical Physics* **147**, 124311 (2017); doi: 10.1063/1.4995997

View online: <http://dx.doi.org/10.1063/1.4995997>

View Table of Contents: <http://aip.scitation.org/toc/jcp/147/12>

Published by the [American Institute of Physics](#)



Scilight

Sharp, quick summaries **illuminating**
the latest physics research

Sign up for **FREE!**

AIP
Publishing

IR + VUV double resonance spectroscopy and extended density functional theory studies of ketone solvation by alcohol: 2-butanone-(methanol)_n, n = 1–4 clusters

Joong-Won Shin^{1,2,a)} and Elliot R. Bernstein^{2,a)}

¹Division of Science, Mathematics, and Technology, Governors State University, University Park, Illinois 60484-0975, USA

²Department of Chemistry, Colorado State University, Fort Collins, Colorado 80523-1872, USA

(Received 13 July 2017; accepted 12 September 2017; published online 29 September 2017)

Infrared plus vacuum ultraviolet (IR + VUV) photoionization vibrational spectroscopy of 2-butanone/methanol clusters [MEK·(MeOH)_n, n = 1–4] is performed to explore structures associated with hydrogen bonding of MeOH molecules to the carbonyl functional group of the ketone. IR spectra and X3LYP/6-31++G(d,p) calculations show that multiple isomers of MEK·(MeOH)_n are generated in the molecular beam as a result of several hydrogen bonding sites available to the clusters throughout the size range investigated. Isomer interconversion involving solvating MeOH rearrangement should probably occur for n = 1 and 2. The mode energy for a hydrogen bonded OH stretching transition gradually redshifts as the cluster size increases. Calculations suggest that the n = 3 cluster isomers adopt structures in which the MEK molecule is inserted into the cyclic MeOH hydrogen bond network. In larger structures, the cyclic network may be preserved. *Published by AIP Publishing.* <https://doi.org/10.1063/1.4995997>

I. INTRODUCTION

Investigation of hydrogen bonding networks in inhomogeneous neutral organic molecular clusters can reveal solvation structures in the vicinity of a highly electronegative functional group. Some of the widely studied inhomogeneous clusters include water/alcohol,^{1–6} water/aromatics,^{7–18} alcohol/aromatics,^{12,15,16,19–24} and other more complicated related systems,^{25,26} for which various hydroxyl-hydroxyl and hydroxyl-aromatic hydrogen bonding interactions are explored using infrared (IR) and/or ultraviolet (UV) spectroscopic methods. Even subtle perturbations caused by the hydrogen bonding interactions in these clusters result in redshifts of OH vibrational stretching energies^{1–26} or change the ππ* electronic transition energies of aromatic groups.^{12,27} These studies indicate that solvation can have a dramatic effect on the physical properties of solute molecules and upon the solvent molecules themselves. The aforementioned work suggests that additional experimental and theoretical analyses of solute-solvent hydrogen bonding interactions involving other hydrogen bond accommodating solute molecules will provide greater insight into the nature of these interactions.

In the current study, infrared plus vacuum ultraviolet (IR + VUV) photoionization vibrational spectroscopy is carried out for 2-butanone-(methanol)_n clusters [(CH₃CH₂C(O)CH₃)·(CH₃OH)_n, MEK·(MeOH)_n, n = 1–4] in order to elucidate hydrogen bonding interactions and solvation structures for MeOH in the vicinity of a carbonyl group. Highly

complicated isomeric structural variation is expected due to the increasing number of hydrogen bonding sites available as the cluster size increases. Structures and redshifts of MeOH OH vibrations are analyzed with density functional theory (DFT) calculations for isomer assignments. Photoionization induced cluster fragmentation pathways are also suggested based upon time of flight (TOF) mass spectrometric results.

II. EXPERIMENTAL PROCEDURE

The experiments are performed at Colorado State University using the apparatus described in detail previously.^{28–31} The MEK·(MeOH)_n, n = 1–4, neutral clusters are generated by supersonic expansion of neat MEK and MeOH liquids in separate reservoirs seeded into a Kr/He mixture (15%/85%, 40 psi backing pressure) using a Jordan Co. pulse valve. A 1 mm aperture diameter skimmer collimates the molecular beam, which is then irradiated by IR and VUV lasers in the ion extraction region of the TOF mass spectrometer.

The VUV radiation (118 nm, ninth harmonic of Nd:YAG fundamental, 10.49 eV, ≤1 μJ/pulse with the conversion efficiency of 1.2 × 10⁻⁵ (Ref. 32)) is generated by excitation of Xe gas in a Xe/Ar mixture (1:10, 200 Torr) using the third harmonic (355 nm, 30 mJ/pulse) of the fundamental beam. Tunable IR radiation (3–5 mJ/pulse in the 2800–3800 cm⁻¹ range with a bandwidth of 2 cm⁻¹) is generated from a N₂ purged optical parametric oscillator/optical parametric amplifier (OPO/OPA) system (LaserVision) pumped by the Nd:YAG fundamental. The IR and VUV beams counterpropagate with respect to one another and are perpendicular to the molecular beam and to the ion flight path.

^{a)}Authors to whom correspondence should be addressed: erb@colostate.edu, Tel.: (970) 491-6347, Fax: (970) 491-1801 and jshin@govst.edu, Tel.: (708) 235-2835, Fax: (708) 534-1641.

In the current study, the IR laser excites neutral cluster OH vibrations about 70 ns prior to VUV ionization so that cluster fragmentation through intermolecular vibrational relaxation results in a population decrease of the absorbing clusters and leads to a dip in mass spectral intensities of product cations. Therefore, IR transitions for the neutral clusters are observed as “negative” IR spectra, whereas enhancements of mass spectral signals indicate IR induced fragmentation of larger clusters into smaller cluster mass channels. The IR spectrum of each neutral species $\text{MEK}\cdot(\text{MeOH})_n$, $n = 2-4$ discussed in the current study is acquired by measuring the ion intensity dip as a function of the IR photon energy at the $\text{MEK}\cdot(\text{MeOH})_x\cdot\text{H}^+$, $x = n - 1$, mass channel. The $\text{MEK}\cdot\text{MeOH}$ neutral cluster can be directly detected at the $m/z = 104$ mass channel.

An IR spectrum of a MeOH molecule is also obtained as a reference for the $\text{MEK}\cdot(\text{MeOH})_n$ cluster spectrum series. VUV ionization products of the molecule in its vibronic ground state cannot be observed because its vertical ionization energy (10.86 eV)³³ is above the photon energy of the ionizing radiation by 0.37 eV; vibrational excitation of the OH group imparts an additional 0.46 eV of energy into the molecule, which makes its ion state accessible through IR assisted VUV photoionization. The excess energy of 0.11 eV following IR + VUV ionization is removed from the molecule as the photoelectron kinetic energy, and observation of the molecular ion MeOH^+ indicates vibrational excitation of the neutral molecule.^{28,30} Each IR spectrum represents a summation of multiple scans in the OH vibration region ($3140-3800\text{ cm}^{-1}$).

III. COMPUTATIONAL METHOD

Calculations are done at Governors State University using the Gaussian 09³⁴ program. Optimized structures and harmonic vibrational frequencies of $\text{MEK}\cdot(\text{MeOH})_n$, $n = 1-3$, cluster isomers are obtained from X3LYP³⁵/6-31++G(d,p)³⁶ calculations, and transition states are calculated using the QST3³⁷ method. The X3LYP extended hybrid functional is employed due to its reported accurate descriptions³⁵ of dispersion, van der Waals, and hydrogen bonding interactions. Basis set superposition error is also minimal for X3LYP calculations.³⁸ Relative structural energy values are zero point corrected, and harmonic vibrational energy values are scaled by the ratio (0.9581) of experimental and theoretical OH stretches of a MeOH molecule.

IV. RESULTS AND DISCUSSION

A. VUV photoionization mass spectrometry

The result of VUV ionization of the supersonic beam of MEK/MeOH vapor is shown in Fig. 1. Ions at $m/z = 65, 97, 129, 161,$ and 193 (indicated in violet) correspond to protonated MeOH clusters, $(\text{MeOH})_x\cdot\text{H}^+$, $x = n - 1$, in the size range $n = 3-7$; these species are products arising from VUV ionization of neutral $(\text{CH}_3\text{OH})_n$ clusters, as has already been identified and assigned in our previous studies^{28,30} of neat MeOH clusters. They are generated by the ionization induced reaction involving the ionization of a methanol oxygen lone pair electron, the transfer of the electron “hole” to the attached

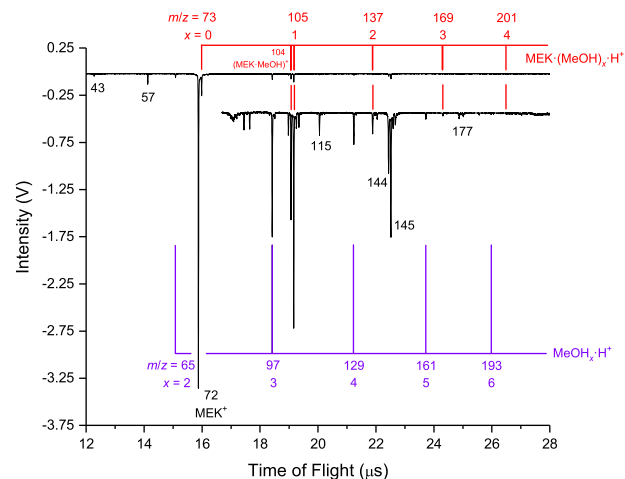
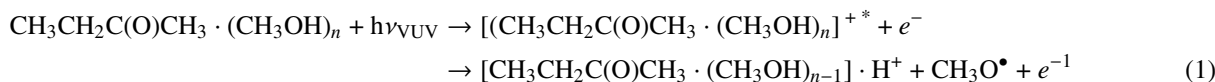


FIG. 1. TOF mass spectrum of VUV ionization products of MEK and MeOH seeded in Kr/He (15%/85%) carrier gas. The mass features identified in violet and red are ionization products of $(\text{MeOH})_n$ and $\text{MEK}\cdot(\text{MeOH})_n$, respectively, and those labeled in black are ionization products of MEK, MEK_2 , and $\text{MEK}_2\cdot\text{MeOH}$. The spectrum in the inset is acquired with the higher mass region expanded vertically. Note that the ion features are identified by $x = n - 1$: they arise according to Eq. (1) in the text. The feature at $m/z = 104$ [$(\text{MEK}\cdot\text{MeOH})^+$] does not fit this pattern: it arises from $\text{MEK}\cdot\text{CH}_3\text{OH}$ neutral cluster without subsequent proton transfer/solvation/loss of $\text{CH}_3\text{O}^\bullet$.

H atom (via electron reorganization), followed by the solvation of the proton by the remaining methanol cluster solvent molecules, with reaction solvation energy sufficient to fragment the $\text{CH}_3\text{O}^\bullet$ neutral radical. As such, these will not be discussed further. Additional mass spectral features include ions appearing at $m/z = 43, 57, 72, 115,$ and 144 (indicated in black). The $m/z = 72$ ion is the molecular ion MEK^+ , and $m/z = 43$ and 57 ions result from the loss of $\text{CH}_3\text{CH}_2^\bullet$ and CH_3^\bullet radical groups, respectively, from MEK^+ . The relative peak intensities of the three ions indicate that the MEK monomer has a stable cation with little photoionization induced fragmentation. The $m/z = 115$ ion corresponds to $\text{MEK}\cdot(\text{CH}_3\text{C}=\text{O})^+$, a fragmentation product of VUV ionization of MEK_2 ($m/z = 144$) through the loss of a $\text{CH}_3\text{CH}_2^\bullet$ radical. Observation of this dimer is interesting in light of the fact that OH groups that lead to stable clusters through hydrogen bond donating interactions are absent. Most likely, the dimer is bound by weak $\text{CH}_3\cdots\text{O}=\text{C}$ interactions.

Ions arising from VUV ionization of $\text{MEK}\cdot(\text{MeOH})_n$ clusters are observed at $m/z = 73, 104, 105, 137, 169,$ and 201 (indicated in red), which correspond to $\text{MEK}\cdot\text{H}^+$, $(\text{MEK}\cdot\text{MeOH})^+$, $\text{MEK}\cdot\text{MeOH}\cdot\text{H}^+$, $\text{MEK}\cdot(\text{MeOH})_2\cdot\text{H}^+$, $\text{MEK}\cdot(\text{MeOH})_3\cdot\text{H}^+$, and $\text{MEK}\cdot(\text{MeOH})_4\cdot\text{H}^+$ clusters, respectively. Both $\text{MEK}\cdot\text{H}^+$ and $(\text{MEK}\cdot\text{MeOH})^+$ ($m/z = 73$ and 104) are the VUV ionization products of neutral $\text{MEK}\cdot(\text{MeOH})_n$ clusters. The detected protonated species $\text{MEK}\cdot(\text{MeOH})_x\cdot\text{H}^+$ are the VUV ionization products of $\text{MEK}\cdot(\text{MeOH})_n$ clusters with $x = n - 1$. As demonstrated in previous work,^{28-32,39,40} one of the solvent molecules in hydrogen bonded clusters undergoes fragmentation (proton transfer from the ionized solvent molecule and solvation of H^+ by the remaining solvent molecules: the negative enthalpy of this reaction is sufficient to fragment the subsequent residual neutral radical, in this instance a CH_3O). This process leads to the formation of protonated cluster ions, with little contribution from larger clusters,



in which $[(\text{CH}_3\text{CH}_2\text{C}(\text{O})\text{CH}_3 \cdot (\text{CH}_3\text{OH})_n)]^{+\ast}$ is the Franck-Condon $\text{MEK} \cdot (\text{MeOH})_n^+$ cation cluster. The reaction leading to the formation of $\text{MEK} \cdot (\text{MeOH})_{n-1}\text{H}^+$ through the loss of a $\text{CH}_3\text{O}^\bullet$ radical from MeOH occurs as the $\text{MEK} \cdot (\text{MeOH})_n^{+\ast}$ Franck-Condon cation relaxes to the ion adiabatic state and releases vibrational energy.

B. IR + VUV photoionization vibrational spectroscopy

Figures 2(a) and 2(b) present a reference MeOH monomer IR spectrum ($m/z=32$ channel) and the IR spectrum of $\text{MEK} \cdot \text{MeOH}$ ($m/z=104$ channel), respectively. The results are summarized in Table I. Unfortunately, a meaningful IR spectrum could not be obtained for the $m/z=73$ channel ($\text{MEK} \cdot \text{H}^+$) because of the inherent fluctuation of the very intense MEK^+ peak ($m/z=72$), which partially overlaps with the weak shoulder $m/z=73$ peak near the baseline, interfered with the acquisition of the spectrum. The OH vibration of the MeOH monomer redshifts from 3685 cm^{-1} to a broad transition centered near 3525 cm^{-1} when the molecule is hydrogen bonded to MEK . The weakly “positive” transition near 3400 cm^{-1} indicates fragmentation as the result of IR absorption of higher order clusters (see Figs. 3 and 5 as discussed below) into the $\text{MEK} \cdot \text{MeOH}$ mass channel. The redshift of 160 cm^{-1} is indicative of a strong hydrogen bond donating motif of the OH group to the O atom in MEK . The redshifted transition is unusually broad for a single hydrogen bonded (i.e., hydrogen bond donating) OH stretch, with the full width at half maximum (FWHM) of 109 cm^{-1} , as obtained from Gaussian fitting. This figure is much greater than that of the single hydrogen bonded OH stretch in $(\text{MeOH})_2$ ($<30\text{ cm}^{-1}$)³⁰ and suggests the presence of multiple isomers of $\text{MEK} \cdot \text{MeOH}$. Figure 2(c) presents X3LYP/6-31++G(d,p) vibrational frequencies of two

representative $\text{MEK} \cdot \text{MeOH}$ isomers, in which MeOH occupies either the ethyl (IA) or methyl (IB) side of the O atom in MEK [Fig. 2(d)]. IB is 0.0269 eV above the global minimum IA, and both of their vibrational frequencies are in agreement with the experimental finding. The broad $\text{MEK} \cdot \text{MeOH}$ transition is not resolved and relative isomer abundances cannot be determined. This observation is in stark contrast with the situations for ethanol,³⁹ 2-propanol,³¹ and butanol⁴¹ dimers, for which the presence of different dimer isomers is evidenced by the observation of distinct, partially resolved hydrogen bonded OH stretch transitions. The variations in OH vibrational energy arise due to different hydrogen bonding motifs in different cluster isomers. The remarkably broad vibrational transition additionally suggests the possibility of dynamic isomerization⁴² of the $\text{MEK} \cdot \text{MeOH}$ cluster while being probed by the IR laser, that is, the $\text{MEK} \cdot \text{MeOH}$ cluster does not adopt a well-defined hydrogen bonding motif. Such motion can lead to a diffuse vibrational energy level. The vibrational energies and structures of the two transition states ($\text{IA-IB}_{\text{trans I}}$ and $\text{IA-IB}_{\text{trans II}}$) connecting the two $\text{MEK} \cdot \text{MeOH}$ minima are shown in Figs. 2(c) and 2(d), respectively. The transition state energies (listed in Table I, 0.0542 and 0.0548 eV) are substantially lower than the experimental OH zero point energy $[(1/2) \cdot h\nu]$ of 0.22 eV . The calculation provides a scenario in which the hydrogen bonded MeOH revolves about the MEK C=O bond axis, and the imaginary frequencies indeed correspond to the MeOH wagging mode about the axis. The OH vibrational frequencies of the transition states are also in agreement with the experimental result. As the O—H bond length and OH \cdots O=C hydrogen bond length constantly change from 0.974 to 0.969 \AA and from 1.896 to 1.957 \AA , respectively, during interconversion, the OH vibrational energy oscillates between

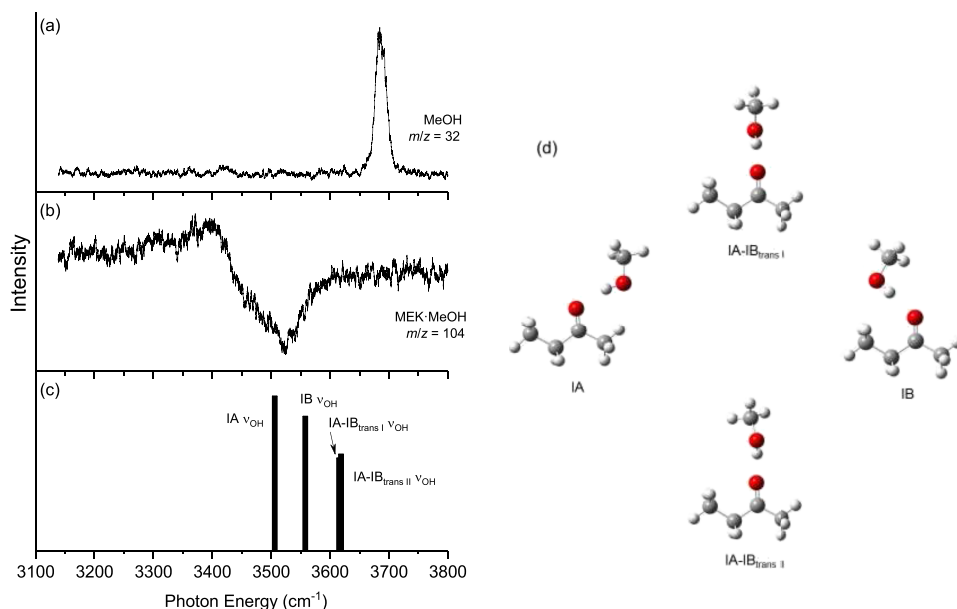
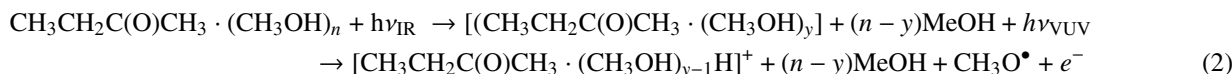


FIG. 2. (a) IR spectrum of MeOH , (b) IR spectrum of $\text{MEK} \cdot \text{MeOH}$, (c) vibrational energies of $\text{MEK} \cdot \text{MeOH}$ isomers and transition states, and (d) structures of $\text{MEK} \cdot \text{MeOH}$ isomers and transition states. The broad transition in the $3450\text{--}3600\text{ cm}^{-1}$ indicates the presence of multiple isomers, and calculations suggest that the cluster undergoes interconversion. The calculations are carried out at X3LYP/6-31++G(d,p), and the vibrational energies are scaled by 0.9581 .

3506 and 3619 cm^{-1} , spanning 113 cm^{-1} , which is very close to the experimental FWHM value of 109 cm^{-1} . Previous studies also suggest that isomers are not locked into specific conformations with defined structures if isomerization barriers are sufficiently low,^{42,43} specifically below the zero point energy of the mode or modes responsible for the isomerization.



in which y indicates that more than one MeOH can be fragmented from the neutral cluster $\text{CH}_3\text{CH}_2\text{C}(\text{O})\text{CH}_3 \cdot (\text{CH}_3\text{OH})_n$ upon absorption of more than one IR photon at high enough laser intensity. The important point here is that the ion signal in the absence of applied IR radiation decreases.

Figure 3 presents the IR spectrum of $\text{MEK} \cdot (\text{MeOH})_2$ obtained at the $m/z = 105$ channel and X3LYP/6-31++G(d,p) structures and vibrational energies of various isomers. The

TABLE I. Experimental OH vibrational stretch energies of $\text{MEK} \cdot (\text{MeOH})_{n=1-4}$, and $\text{MEK} \cdot (\text{MeOH})_{n=1-3}$ isomer relative structural energies and harmonic OH vibrational stretch energies. Structural energies (ΔE_{ZPE}) are zero point corrected, and the calculated vibrational energies are scaled by 0.9581. Calculations are carried out at the X3LYP/6-31++G(d,p) level. OH vibrational stretch energy of a MeOH molecule is shown as a reference.

$\text{MEK} \cdot \text{MeOH}_n$, n	Ion m/z	Expt. ν_{OH} (cm^{-1})
MeOH	32	3685
1	104	3525
2	105	3441, 3455, 3491, 3514
3	137	3419 ^a
4	169	3269 ^a
Isomer	ΔE_{ZPE} (eV)	Calc. ν_{OH} (cm^{-1})
IA	0.0000	3506
IB	0.0269	3558
IA-IB _{trans} I	0.0542	3619
IA-IB _{trans} II	0.0548	3616
IIA	0.0000	3382, 3430
IIB	0.0237	3414, 3517
IIC	0.0650	3418, 3616
IID	0.1612	3537, 3574
IIA-IID _{trans}	0.1794 ^b	3612, 3617
IIC-IID _{trans}	0.1236 ^c	3509, 3653
IIIA	0.0000	3276, 3364, 3434
IIIB	0.0172	3311, 3367, 3434
IIIC	0.1698	3439, 3498, 3541
IIID	0.1846	3402, 3499, 3603

^aEstimated center of the peak from Gaussian fitting.

^bWith respect to IIA.

^cWith respect to IIC.

The general reaction/detection scheme for neutral $\text{MEK} \cdot (\text{MeOH})_n$ cluster IR spectra is similar to that above given in Eq. (1) with the addition of IR photons to be absorbed by the neutral species with the loss of an MeOH molecule, which results in a decrease of the signal in the $\text{MEK} \cdot (\text{MeOH})_{n-1} \cdot \text{H}^+$ mass channel,

stretching mode associated with the hydrogen bonded OH moiety is observed in the 3425–3575 cm^{-1} range and, similar to the case for $\text{MEK} \cdot \text{MeOH}$, the broad transition indicates that several isomeric structures of $\text{MEK} \cdot (\text{MeOH})_2$ are present. The isomeric variation in the hydrogen bonding network in $\text{MEK} \cdot (\text{MeOH})_n$ clusters is similar to that shown in two photon ionization⁴⁴ and computational⁴⁵ studies of styrene- $(\text{MeOH})_n$ clusters. The bands are much broader than those observed for $(\text{MeOH})_2$,³⁰ implying interconversion among an increased number of isomers. Four representative $\text{MEK} \cdot (\text{MeOH})_2$ isomeric structures are obtained from the calculations, three linear structures in which the second MeOH molecule is hydrogen bonded to the first one (IIA, IIB, and IIC) and another structure in which it is hydrogen bonded to the O atom of MEK (IID). All of the calculated OH vibrational energies of these clusters are within the broad vibrational envelope, and for IIA, IIB, and IIC, the lower energy features correspond to the OH vibration of the donor MeOH, while the higher energy features correspond to those of the acceptor-donor MeOH. In IID, the vibrational energies are similar to those for IA and IB as the OH vibration on the methyl side of MEK is predicted at a lower energy than that on the ethyl side. The transition states for the IIA-IID and IIC-IID pairs are located with the barriers of 0.1794 and 0.1236 eV, respectively, which are higher than the IA-IB interconversion barriers, but still below the experimental OH zero point energy of 0.22 eV. Transition states for IIA-IIB, IIA-IIC, IIB-IIC, and IIB-IID interconversion are not located despite extensive QST3 searches. Thus, while interconversion among different isomers is a possibility, which can generate a broad absorption band as observed, one cannot draw any firm conclusions from these theoretical results concerning the comparative nature of the observed spectra for these isomers.

Figure 4 shows the IR spectrum of neutral $\text{MEK} \cdot (\text{MeOH})_3$ obtained at mass channel $m/z = 137$, $[\text{MEK} \cdot (\text{MeOH})_2 \cdot \text{H}^+]$, X3LYP/6-31++G(d,p) isomer structures, and their respective vibrational energies. The broad redshifted hydrogen bonded OH stretching band in the 3200–3600 cm^{-1} region is indicative of the onset of condensed phase like behavior of hydrogen bonded clusters. The broad transition is similar to vibrational features observed^{28-31,41,46} in cyclic alcohol clusters, for which each MeOH is both a hydrogen bond donor and acceptor. Calculations show that linear $\text{MEK} \cdot (\text{MeOH})_3$ isomer structures (IIIA and IIIB) are the lowest in energy with IIIA being

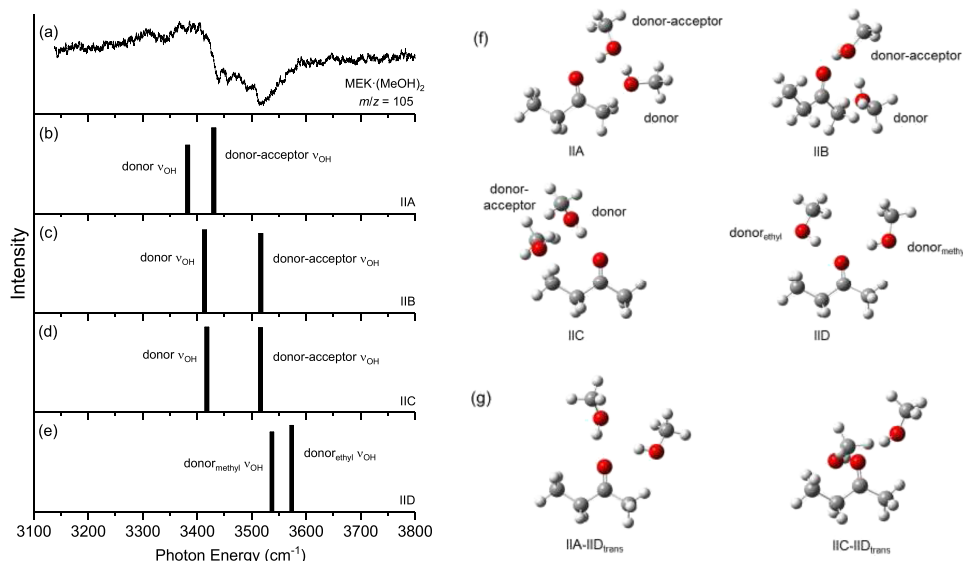


FIG. 3. (a) IR spectrum of $\text{MEK} \cdot (\text{MeOH})_2$, detected at $m/z = 105$ [$\text{MEK} \cdot \text{MeOH} \cdot \text{H}^+$], (b)–(e) calculated vibrational energies of $\text{MEK} \cdot (\text{MeOH})_2$ isomers, (f) representative structures of $\text{MEK} \cdot (\text{MeOH})_2$ isomers, and (g) structures of $\text{MEK} \cdot (\text{MeOH})_2$ interconversion transition states. The broad transition in the $3425\text{--}3575$ cm^{-1} range indicates the presence of multiple isomers. The calculations are carried out at X3LYP/6-31++G(d,p), and the vibrational energies are scaled by 0.9581.

the global minimum and IIB being slightly less stable at the relative energy of 0.0172 eV: their calculated vibrational energies are in excellent agreement with the experimental results. The highest and lowest vibrational energies correspond to the OH vibrations of the two donor-acceptor MeOHs (labeled α and β), whereas the vibrational energy predicted to fall between these two donor-acceptor modes corresponds to the donor MeOH vibration. Both structures (α and β) adopt a geometry in which MEK is inserted into the cyclic hydrogen bonding network of a MeOH trimer, with the cyclic arrangement partially preserved. In the two other higher energy clusters (IIC and IID), the cyclic arrangement is not preserved, and their vibrational energies are only in marginal agreement

with the experimental result. We did not locate a structure in which the planar cyclic arrangement of the MeOH trimer is fully preserved.

The IR spectrum of the large cluster $\text{MEK} \cdot (\text{MeOH})_4$ is presented in Fig. 5. The broad envelop in the $3200\text{--}3600$ cm^{-1} region suggests condensed phase behavior with multiple stable isomers present with all OH groups involved in a complex hydrogen bonding network. Based on the result for $\text{MEK} \cdot (\text{MeOH})_3$ and previous results^{31,47} that cyclic alcohol clusters are the most stable ones in the gas phase, larger $\text{MEK} \cdot (\text{MeOH})_n$ clusters may adopt a geometry that contains cyclic methanol cluster moieties as has been suggested for large styrene· $(\text{MeOH})_n$ clusters.⁴⁵

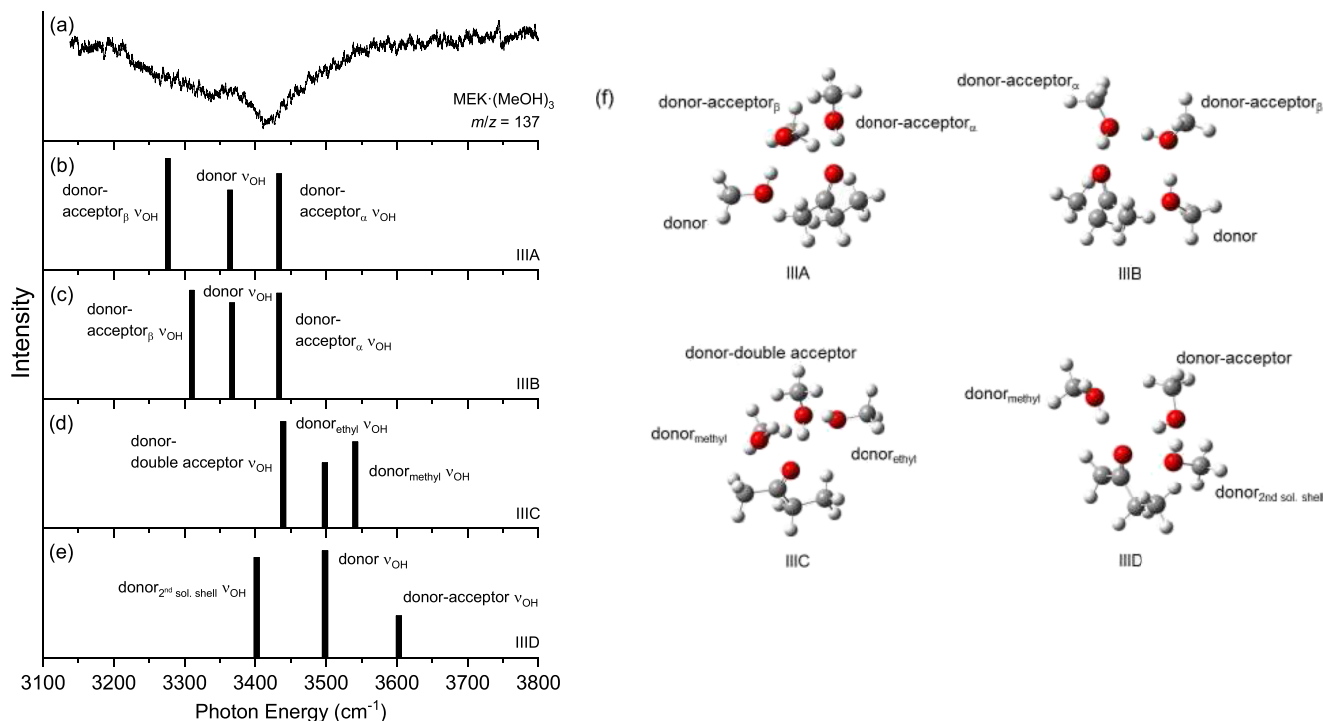


FIG. 4. (a) IR spectrum of $\text{MEK} \cdot (\text{MeOH})_3$, detected at the $m/z = 137$ [$\text{MEK} \cdot (\text{MeOH})_2 \cdot \text{H}^+$], (b)–(e) calculated spectra of $\text{MEK} \cdot (\text{MeOH})_3$ isomers, and (f) representative structures of $\text{MEK} \cdot (\text{MeOH})_3$ isomers. The broad transition in the $3200\text{--}3575$ cm^{-1} range indicates the presence of multiple isomers. The calculations are carried out at X3LYP/6-31++G(d,p), and the vibrational energies are scaled by 0.9581.

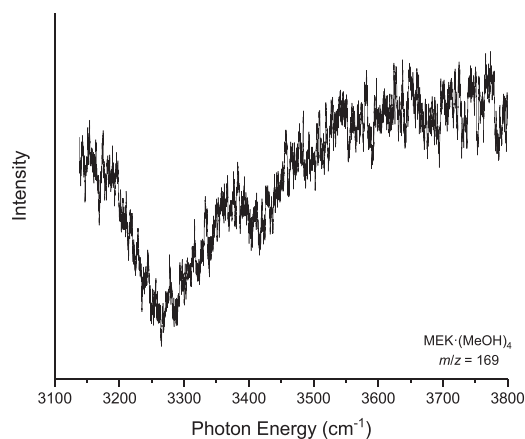


FIG. 5. IR spectrum of $\text{MEK}\cdot(\text{MeOH})_4$, detected at $m/z = 167$ [$\text{MEK}\cdot(\text{MeOH})_3\cdot\text{H}^+$]. The broad transition in the $3150\text{--}3500\text{ cm}^{-1}$ region indicates an extensive hydrogen bonding network. The hydrogen bonded OH stretch band does not redshift as the cluster size increases from $n = 3$ in Fig. 4 to $n = 4$, suggesting condensed phase behavior of the solvating MeOH in this cluster size range.

V. CONCLUSIONS

IR + VUV photoionization vibrational spectroscopy of $\text{MEK}\cdot(\text{MeOH})_n$, $n = 1\text{--}4$, has been carried out to study hydrogen bonding structures of a ketone solvation by MeOH molecules. VUV ionization of MEK and MeOH seeded in a Kr/He carrier gas generates MEK^+ , $(\text{MEK}\cdot\text{MeOH})^+$, and $\text{MEK}\cdot(\text{MeOH})_{n-1}\cdot\text{H}^+$ cations. IR + VUV spectra and X3LYP/6-31++G(d,p) calculations show that multiple neutral cluster isomers are generated under the current experimental conditions, resulting in broad hydrogen bonded OH stretch transitions. In the case of $\text{MEK}\cdot\text{MeOH}$, MeOH is hydrogen bonded to the O atom of MEK and revolves around the $\text{C}=\text{O}$ bond axis, yielding a hydrogen bonded OH stretch that is much broader than that of the $(\text{MeOH})_2$ cluster.^{28,30} $\text{MEK}\cdot(\text{MeOH})_2$ also yields a broad OH transition originating from the presence of several isomers; however, unlike the situation for $\text{MEK}\cdot\text{MeOH}$, transition states for the $\text{MEK}\cdot(\text{MeOH})_2$ isomer interconversions are not clearly identified. The onset of condensed phase like features is observed for $\text{MEK}\cdot(\text{MeOH})_3$: this cluster shows a broad hydrogen bonded OH transition that is highly reminiscent of that for cyclic alcohol trimers. Calculations yield that the most stable $\text{MEK}\cdot(\text{MeOH})_3$ structures adopt a linear geometry in which the MEK is inserted into the cyclic hydrogen bond network of $(\text{MeOH})_3$. We also suggest that larger clusters may have structures in which the MEK is bound to a cyclic hydrogen bond network of MeOH molecules.

ACKNOWLEDGMENTS

This work is supported by the US Army Research Office (No. W911NF-10-1-0117) for Colorado State University and in part by the Division of Chemistry and Biological Sciences (currently the Division of Science, Mathematics, and Technology) at Governors State University.

¹Y.-C. Tse, M. D. Newton, and L. C. Allen, *Chem. Phys. Lett.* **75**, 350 (1980).

²W. L. Jorgensen, *J. Phys. Chem.* **90**, 1276 (1986).

- ³F. Huisken and M. Stemmler, *Chem. Phys. Lett.* **180**, 332 (1991).
- ⁴N. Bakkas, Y. Bouteiller, A. Loutellier, J. P. Perchard, and S. Racine, *J. Chem. Phys.* **99**, 3335 (1993).
- ⁵N. Bakkas, Y. Bouteiller, A. Loutellier, J. P. Perchard, and S. Racine, *Chem. Phys. Lett.* **232**, 90 (1995).
- ⁶P. A. Stockman, G. A. Blake, F. J. Lovas, and R. D. Suenram, *J. Chem. Phys.* **107**, 3782 (1997).
- ⁷A. J. Gotch and T. S. Zwier, *J. Chem. Phys.* **96**, 3388 (1992).
- ⁸M. Schütz, T. Bürgi, and S. Leutwyler, *J. Mol. Struct.: THEOCHEM* **276**, 117 (1992).
- ⁹R. N. Pribble and T. S. Zwier, *Science* **265**, 75 (1994).
- ¹⁰R. N. Pribble, A. W. Garrett, K. Haber, and T. S. Zwier, *J. Chem. Phys.* **103**, 531 (1995).
- ¹¹S. Y. Fredericks, K. D. Jordan, and T. S. Zwier, *J. Phys. Chem.* **100**, 7810 (1996).
- ¹²A. Mitsuzuka, A. Fujii, T. Ebata, and M. Mikami, *J. Chem. Phys.* **105**, 2618 (1996).
- ¹³P. Tarakeshwar, H. S. Choi, S. J. Lee, J. Y. Lee, K. S. Kim, T.-K. Ha, J. H. Jang, J. G. Lee, and H. Lee, *J. Chem. Phys.* **111**, 5838 (1999).
- ¹⁴R. C. Guedes, B. J. C. Cabral, J. A. M. Simoes, and H. P. Diogo, *J. Phys. Chem. A* **104**, 6062 (2009).
- ¹⁵Y. Matsumoto, T. Ebata, and N. Mikami, *J. Phys. Chem. A* **105**, 5727 (2001).
- ¹⁶H. Mahmoud, I. N. Germanenko, Y. Ibrahim, and M. S. El-Shall, *Chem. Phys. Lett.* **356**, 91 (2002).
- ¹⁷Y. Nibu, R. Marui, and H. Shimada, *J. Phys. Chem. A* **110**, 9627 (2006).
- ¹⁸M. Sugiyama, H. Ishikawa, W. Setaka, M. Kira, and N. Mikami, *J. Phys. Chem. A* **112**, 1168 (2008).
- ¹⁹N. Guchhait, T. Ebata, and N. Mikami, *J. Phys. Chem. A* **104**, 11891 (2000).
- ²⁰M. Sakai, K. Daigoku, S.-I. Ishiuchi, M. Saeki, K. Hashimoto, and M. Fujii, *J. Phys. Chem. A* **105**, 8651 (2001).
- ²¹H. Yokoyama, H. Watanabe, T. Omi, S.-I. Ishiuchi, and M. Fujii, *J. Phys. Chem. A* **105**, 9366 (2001).
- ²²Y. Matsumoto, T. Ebata, and N. Mikami, *J. Phys. Chem. A* **106**, 5591 (2002).
- ²³V. Venkatesan, A. Fujii, T. Ebata, and N. Mikami, *J. Phys. Chem. A* **109**, 915 (2005).
- ²⁴P. C. Singh, B. Bandyopadhyay, and G. N. Patwari, *J. Phys. Chem. A* **112**, 3360 (2008).
- ²⁵A. W. Garrett, T. S. Zwier, and D. L. Severance, *J. Phys. Chem.* **96**, 9710 (1992).
- ²⁶F. C. Hagemeister, C. J. Gruenloh, and T. S. Zwier, *Chem. Phys.* **239**, 83 (1998).
- ²⁷H. Abe, N. Mikami, and M. Ito, *J. Phys. Chem.* **86**, 1768 (1982).
- ²⁸H. B. Fu, Y. J. Hu, and E. R. Bernstein, *J. Chem. Phys.* **124**, 024302 (2006).
- ²⁹Y. J. Hu, H. B. Fu, and E. R. Bernstein, *J. Chem. Phys.* **125**, 154305 (2006).
- ³⁰Y. J. Hu, H. B. Fu, and E. R. Bernstein, *J. Chem. Phys.* **125**, 154306 (2006).
- ³¹J.-W. Shin and E. R. Bernstein, *J. Chem. Phys.* **130**, 214306 (2009).
- ³²Y. J. Shi, S. Consta, A. K. Das, B. Mallik, D. Lacey, and R. H. Lipson, *J. Chem. Phys.* **116**, 6990 (2002).
- ³³F. M. Benoit and A. G. Harrison, *J. Am. Chem. Soc.* **99**, 3980 (1977).
- ³⁴M. J. Frisch, G. W. Trucks, H. B. Schlegel *et al.*, GAUSSIAN 09, Revision C.01, Gaussian, Inc., Wallingford, CT, 2009.
- ³⁵X. Xu and W. A. Goddard III, *Proc. Natl. Acad. Sci. U. S. A.* **101**, 2673 (2004).
- ³⁶G. A. Petersson, A. Bennett, T. G. Tensfeldt, M. A. Al-Laham, W. A. Shirley, and J. Mantzaris, *J. Chem. Phys.* **89**, 2193 (1988).
- ³⁷C. Peng, P. Y. Ayala, H. B. Schlegel, and M. J. Frisch, *J. Comput. Chem.* **17**, 49 (1996).
- ³⁸J. T. Su, X. Xu, and W. A. Goddard III, *J. Phys. Chem. A* **108**, 10518 (2004).
- ³⁹G. S. Fanourgakis, Y. J. Shi, S. Consta, and R. H. Lipson, *J. Chem. Phys.* **119**, 6597 (2003).
- ⁴⁰S.-T. Tsai, J.-C. Jiang, M.-F. Lin, Y. T. Lee, and C.-K. Ni, *J. Chem. Phys.* **120**, 8979 (2004).
- ⁴¹R. A. Provencal, R. N. Casaes, K. Roth, J. B. Paul, C. N. Chapo, R. J. Saykally, G. S. Tschumper, and H. F. Schaefer III, *J. Phys. Chem. A* **104**, 1423 (2000).

- ⁴²W. H. Robertson, E. A. Price, J. M. Weber, J.-W. Shin, G. H. Weddle, and M. A. Johnson, *J. Phys. Chem. A* **107**, 6527 (2003).
- ⁴³P. J. Breen, J. A. Warren, E. R. Bernstein, and J. I. Seeman, *J. Chem. Phys.* **87**, 1917 (1987).
- ⁴⁴H. Mahmoud, I. N. Germanenko, Y. Ibrahim, and M. S. El-Shall, *J. Phys. Chem. A* **107**, 5920 (2003).
- ⁴⁵M. S. El-Shall, D. Wright, Y. Ibrahim, and H. Mahmoud, *J. Phys. Chem. A* **107**, 5933 (2003).
- ⁴⁶R. A. Provencal, J. B. Paul, K. Roth, C. Chapo, R. N. Casaes, R. J. Saykally, G. S. Tschumper, and H. F. Schaefer III, *J. Chem. Phys.* **110**, 4258 (1999).
- ⁴⁷D. Wright and M. S. El-Shall, *J. Chem. Phys.* **105**, 11199 (1996).